Intermediate structure resonances in the inelastic scattering of ^{12}C on ^{16}O†

R. E. Malmin,* J. W. Harris, and P. Paul
Department of Physics, State University of New York, Stony Brook, New York 11794
(Received 30 November 1977)

Excitation functions for inelastic scattering of $^{12}C + ^{16}O$ to the 2^+ state in ^{12}C at 4.43 MeV, the $(3^-,0^+)$ doublet at 6.1 MeV and the $(2^+,1^-)$ states at 7.0 MeV in ^{16}O have been measured over the energy range $33 \leq E_{lab} \leq 54$ MeV in 200-keV steps, at c.m. angles ranging from 100° to 165°. Several new intermediate structure resonances are observed in the inelastic channels. A statistical analysis reveals strong correlations in angle and in exit channels. Complete elastic and inelastic angular distributions were measured at the energies of $E_{c.m.} = 13.6$, 19.7, 20.5, 22.0, and 22.6 MeV as well as as at 21.3 MeV. Optical model fits to the elastic angular distributions result in the spin assignments $J = 9^-$, 14^+, and 15^- (16^+) for the resonances at $E_{c.m.} = 13.6$, 19.7, and 22.0 MeV, respectively. Partial widths are extracted from the data. The reduced widths of the inelastic channels are large, establishing their importance in the resonance mechanism. The results are compared to predictions of existing models, and it is found that a simple double-resonance model does not adequately describe the data.

[NUCLEAR REACTIONS $^{12}C(^{16}O, ^{16}O^*)^{12}C^*$; $E = 33-54$ MeV, $\theta_{c.m.} = 100°-160°$; measured $\sigma(E,\theta)$, deduced resonances, J, reduced widths.]

I. INTRODUCTION

Resonances in heavy ion reactions were first observed in sub-Coulomb barrier reactions as narrow structures correlated in energy in all open channels of the $^{12}C + ^{12}C$ system.[1] Similar resonant structure was also observed below the Coulomb barrier in the $^{12}C + ^{16}O$ system.[2] Data on these subbarrier systems have since been extended[3-7] and numerous other resonances have been identified. Extensive investigation of other systems[8-10] has failed to yield clearcut evidence to support the existence of subbarrier resonances in systems other than $^{12}C + ^{12}C$ and $^{12}C + ^{16}O$.

Single particle models[11-13] describing these states as quasibound levels in the ion-ion potential found it difficult to account for the narrow widths *and* large number of observed levels. A more general reaction mechanism was necessary to describe the resonances, i.e., the incident channel must couple to other more complex and longer lived degrees of freedom of the resonant system. The molecular model introduced by Imanishi[14] takes into account strong coupling of elastic and inelastic amplitudes in the incident channel. As extended by Kondo[15] to include simultaneous excitation in both ^{12}C nuclei this model has been able to reproduce a large number of resonant energies and spins observed in the $^{12}C + ^{12}C$ system.[7]

The presence of resonances in some systems, notably those considered to be good α-particle nuclei, and their absence in others led Michaud and Vogt[16] to propose an α-cluster model. In this model the resonances correspond to complex α-cluster configurations rather than "dinuclear" resonances. The more complex spatial geometry introduces additional degrees of freedom but the predictions so far are only qualitative.[17]

At energies above the Coulomb barrier nonstatistical resonance phenomena were first observed by Halbert *et al.*,[18] who reported an anomaly at 13.7 MeV (c.m.) in the $^{12}C(^{16}O, \alpha)^{24}Mg$ reaction. This resonance was subsequently observed in the elastic scattering[19,20] along with an even more prominent structure at 19.7 MeV. Angular distributions at the latter resonance[20] indicated a spin of $J = 14^+$ while just off-resonance the pattern is dominated by $J = 13$. Experiments at Argonne,[20] Yale,[21] Brookhaven,[22] and Munich[23] have shown that this resonance is correlated in several inelastic channels and in selective highly excited proton and neutron channels.

The observed width ($\Gamma \sim 380$ keV) is intermediate between the single particle value ($\Gamma_{s.p.} \sim 1.5$ MeV) estimated[24] using the empirical[20,25] $^{12}C + ^{16}O$ optical potential and the average coherence width ($\Gamma_{CN} \sim 120$ keV) of the underlying compound nucleus fluctuations.[25,26] Reasonable estimates[27] of the level density at 36.5 MeV in ^{28}Si yield $\rho(J^\pi = 14^+) \sim 30^{+30}_{-20}$ states/MeV. Thus the observed resonance probably involves many compound levels. These factors suggest interpretations in terms of intermediate structure and doorway states.[28]

Several possible mechanisms have been proposed to explain the resonance at $E_{c.m.} = 19.7$ MeV in the $^{12}C + ^{16}O$ system. Essentially the same as those used to describe sub-Coulomb barrier resonances, they include the coupled channels model of Imanishi,[14] the very similar "double-

resonance" model of Scheid *et al.*,[29] and the α-cluster model of Michaud and Vogt.[16] In the spirit of the latter model, a resonance mechanism involving the elastic transfer of an α particle between identical ^{12}C cores has also been proposed.[21]

On the other hand, Moldauer[30] pointed out that a proper R-matrix statistical model treatment in the presence of strong absorption yields features very similar to those observed and predicted by intermediate structure or doorway state models. Where there is a limited number of competing open channels under the influence of strong absorption, this model predicts a much broader distribution of resonance pole widths and strengths than expected from the usual Ericson model.[31] As a result, a few widths are observed to have values much larger than average even when $\langle\Gamma\rangle/D \gg 1$. Since large resonance amplitudes are usually associated with large widths, it is expected that such a strong intermediate resonance in the entrance channel will also be observed in several exit channels. Likewise, this model predicts that the resonance will be characterized by a well-defined angular momentum in each channel resulting in a characteristic angular distribution. Such resonances are expected to be observed strongly in the elastic scattering of heavy ions due to the strong absorption.

With the presence of such distinctive models and in the absence of enough intermediate structure resonance information to distinguish between the proposed mechanisms in these reactions, an extensive search for systematic intermediate structure resonances in the $^{16}O+^{12}C$ system was initiated sometime ago at Stony Brook. This system allows even and odd parity states and we chose to investigate the inelastic channels for the following reasons. Although the compound elastic contribution is small[25] ($\leq$15%), it is sufficient to obscure all but a very strong resonance in the entrance channel. Observed correlations in the neutron,[23] proton,[22] deuteron,[23] and α (Refs. 21 and 26) channels are at best weak and limited to a few selected levels at high excitation. However, excitation functions over a limited energy range[20] near $E_{\text{c.m.}}=19.7$ MeV show a strong resonance in the inelastic scattering to the doublet of states at 6.1 MeV excitation in ^{16}O which is correlated at all six measured angles. Finally, simple calculations employing the empirically determined $^{12}C+^{16}O$ potential readily produce a resonance in the $l=14$ partial wave within several hundred keV of the observed resonance at 19.7 MeV, and indicate that energy and angular momentum matching conditions are favorable for the double-resonance model over a broad range of incident energies.

Thus we investigated inelastic scattering to low-lying states in ^{12}C and ^{16}O to search for new intermediate structure resonances in the $^{12}C+^{16}O$ system which might be obscured in the elastic channel by fluctuations. Such resonance information on the inelastic channels will provide important information with which to test the proposed reaction mechanisms. Detailed excitation functions for several inelastic channels as well as the elastic channel were measured over a large range of center-of-mass energies. Elastic angular distributions were then taken at prospective resonant energies in order to determine the spins of the observed resonances. Inelastic angular distributions were also measured at these energies in order to provide total cross sections for determining the importance of each inelastic channel in the observed resonance. Preliminary reports of the present work have been presented elsewhere.[32]

II. EXPERIMENTAL PROCEDURE

An ^{16}O beam from the Stony Brook FN tandem Van de Graaff was used to bombard self-supporting C foils of 20–100-$\mu g/cm^2$ areal density. Elastically and inelastically scattered ^{16}O ions and ^{12}C recoils were detected in a pair of ΔE-E particle telescopes mounted 15° apart in a standard 76-cm Ortec scattering chamber. The ΔE detectors were 12 and 15 μm thick. Total energy ($E+\Delta E$) and corresponding particle identification ($E\times\Delta E$) pulses generated with a standard pulse multiplication circuit were stored on-line in a PDP-9 computer. Final particle identification gates were set digitally on-line. A single channel analyzer monitoring the PI output of the forward-most detector was used to "prescale" the gates for small angle oxygen scattering by factors from 1/1 to 1/1000 to reduce computer deadtime. Deadtime corrections, made by comparing total computer gates to the integral of the two PI spectra, were normally $\leq$10%. The energy resolution, determined chiefly by target thickness and kinematic broadening ($dE/d\theta \approx 1$ MeV/deg), was sufficient to separate the doublet at 6.1 MeV excitation in ^{16}O from the doublet at 7.0 MeV but not to resolve individual members of either doublet. A typical spectrum appears in Fig. 1. The angular accuracy of the detectors was especially important in angular distribution measurements since $d\theta(\text{c.m.})/d\theta(\text{lab}) \geq 2$. This was found to be very sensitive to chamber alignment and beam collimation. Therefore the beam was tightly collimated by a set of 1.6×6.4-mm collimators ~ 60 cm apart and chamber alignment

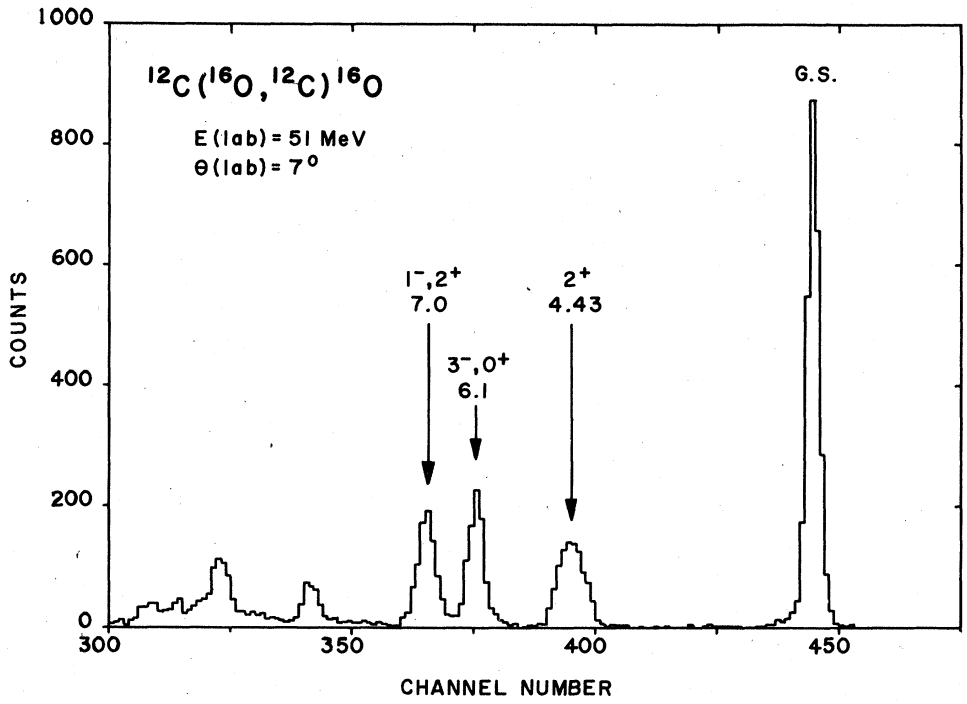

FIG. 1. Typical spectrum of ^{12}C recoils from $^{12}C(^{16}O, ^{12}C)^{16}O$ reaction.

was checked with beam to be accurate to $<0.1°$. Detector collimators subtended a half angle of $\pm 0.25°$ and a solid angle of $\simeq \frac{1}{4}$ msr.

Relative normalization between detectors was determined geometrically and checked by overlapping data points. The relative yields in the excitation functions were determined from the integrated beam currents. The angular distributions were normalized to a monitor counter. Absolute cross sections were determined by normalizing to Rutherford scattering and compared with previously published results.[20,25] Relative cross sections are estimated to be accurate to $\pm 5\%$ while the absolute cross sections are accurate to better than 15%.

III. EXPERIMENTAL RESULTS

A. Excitation functions

Detailed excitation functions were measured for elastic scattering and inelastic scattering to the 2^+ state at 4.43 MeV in ^{12}C, the $(3^-, 0^+)$ doublet at 6.1 MeV and the $(2^+, 1^-)$ doublet near 7.0 MeV in ^{16}O. The data cover a laboratory energy range from $\simeq$33 to 54 MeV in 200-keV steps and a center-of-mass angular range of $\simeq$100 to 150°. Inelastic scattering data were limited to backward angles in the center of mass obtained by detecting the forward scattered ^{12}C recoils. The low energy cutoff of these data ($\simeq$33 MeV) was determined by the point below which the inelastically scattered ^{12}C ions could no longer penetrate the ΔE detectors. In addition, excitation functions were obtained over a more limited laboratory energy range from 45 to 56 MeV in 300-keV steps at a center-of-mass angle of $\simeq 166°$ corresponding to 7° in the lab.

The excitation function data for the elastic scattering are shown in Fig. 2. The data are characterized by an underlying gross structure $\simeq$1.5 MeV in width with considerable statistical fluctuations superimposed, and are essentially identical to the data of Ref. 20. A statistical analysis[25] of that data extracted an average coherence width $\langle \Gamma_{CN} \rangle$ of 115 keV. While that analysis determined that the reaction process was $\geq 85\%$ direct even at backward angles, the resulting fluctuations obscure all but the very strong $J = 14^+$ resonance visible in Fig. 2 at $E_{c.m.} = 19.7$ MeV. Figure 3 shows the deviation from the average cross section as a function of energy summed over all angles for the data of Ref. 20. Here the 19.7-MeV resonance stands out quite strongly, as does the resonance at 13.6 MeV. It would be difficult, however, to distinguish weaker resonances from the fluctuations.

Excitation functions for the inelastic scattering to the $(3^-, 0^+)$ doublet at 6.1 MeV in ^{16}O are displayed in Fig. 4. The most striking feature of these data are two pairs of resonant "doublets," one set at (19.7, 20.5) MeV, and another at (22.0,

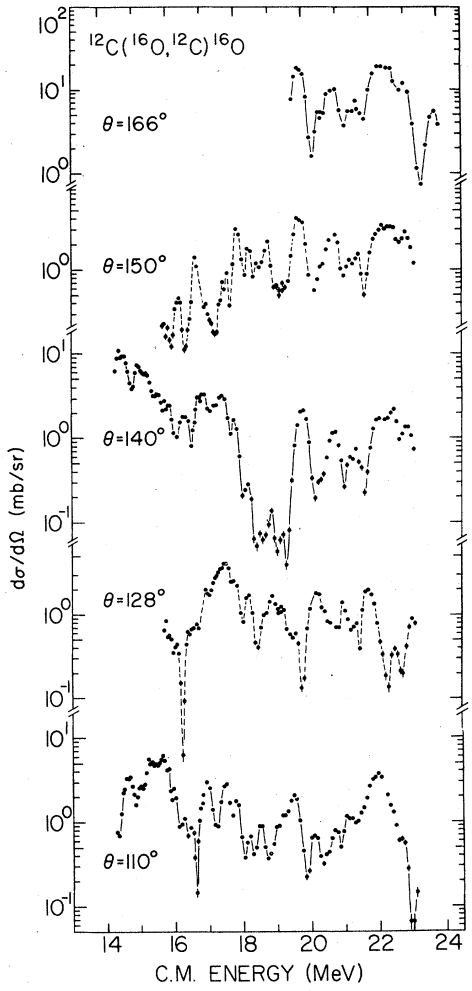

FIG. 2. Excitation functions for ^{12}C and ^{16}O elastic scattering.

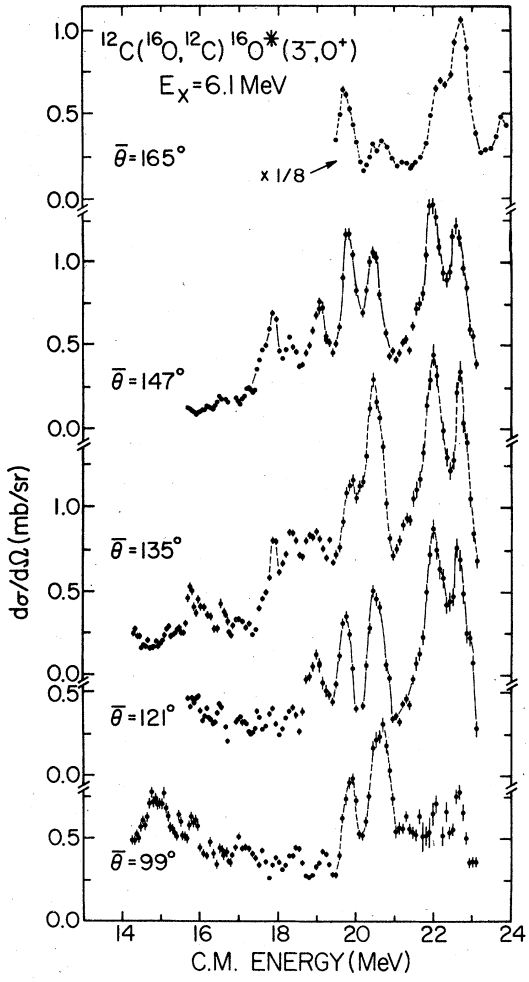

FIG. 4. Excitation functions for ^{12}C and ^{16}O inelastic scattering to $(0^{+}, 3^{-})$ doublet at 6.1 MeV excitation in ^{16}O.

22.6) MeV. The lower member of the first "doublet" appears at the same energy as the 14^{+} resonance seen in the elastic scattering. The lower member of the second "doublet" is correlated with the third largest, albeit weak peak in the correlation function of Fig. 3. The widths of these resonances are all ≃400–500 keV, which is a factor of 3 larger than the underlying compound nuclear widths and a factor of 3 to 4 narrower than the single particle width. There is considerably weaker evidence for correlated peaks at 17.9 and 19.0 MeV and possibly at 15.9 and 16.5 MeV.

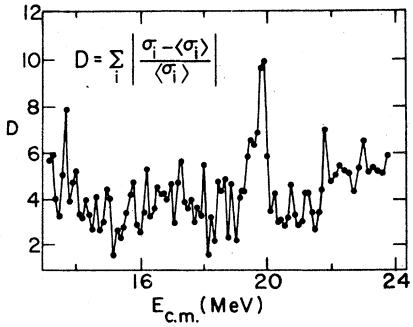

FIG. 3. Angle-integrated correlation function D indicating deviations from the mean cross section (taken from Ref. 20).

Another striking feature of these data is the high degree of angular cross correlation. Figure 5 shows the 6.1-MeV excitation functions at two angles ≃26° apart (the coherence angle ≃6°). Not only are the resonances strongly correlated, but in the region of the resonances, every peak and valley in one curve is reflected in the other.

Excitation functions for the 2^{+} state at 4.43 MeV in ^{12}C are shown in Fig. 6. The systematic "doublets" so prominent in the 6.1-MeV data are

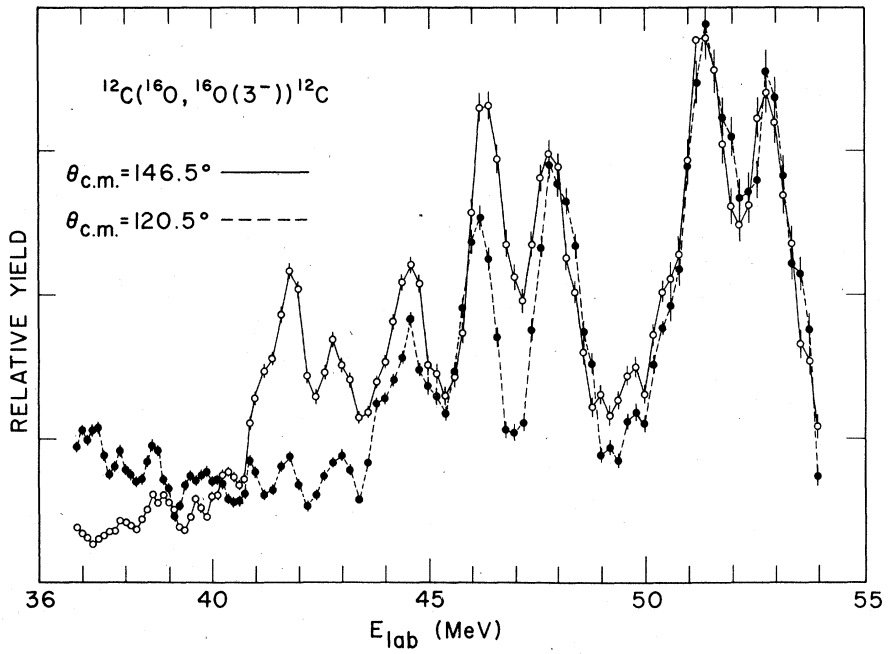

FIG. 5. The 6.1-MeV excitation function data at two angles 26° (c.m.) apart. The coherence angle is ~ 6°.

not evident in these data. However, there is a very strong correlated peak at 22.6 MeV, the same energy as the highest energy peak observed in the 6.1-MeV data. The next lower energy peak at 22.0 MeV observed in the 6.1-MeV data is conspicuously absent, or perhaps shifted down in energy. There is a sharp minimum in the 2^+ cross section at 19.7 MeV, though there appear to be correlated peaks at both 19.9 and 21.7 MeV, and possibly at 19.4 MeV. There is no convincing evidence, however, for a strong peak at 20.5 MeV.

Figure 7 presents the results for the $(2^+, 1^-)$ doublet at 7.0 MeV in ^{16}O. Here the data are somewhat smeared out, probably indicating that both states are contributing. There is clearly a strong, but somewhat washed out "doublet" of peaks centered again at 22.0 and 22.6 MeV. In fact, the 22.0-MeV peak is seen to dominate at forward angles giving way to the 22.6-MeV component at backward angles. At 19.7 MeV there is a weak, correlated peak and possibly others at 19.4, 20.8, and 21.6 MeV.

B. Results of statistical analysis

A standard Ericson statistical fluctuation analysis[31] was performed on the inelastic scattering data. The method and computer codes used were identical to those of Ref. 26. Appropriate corrections[33] have been made for the effects of energy resolution, averaging interval (~1.2 MeV), and the finite range of the data. The average coherence width of the underlying compound levels, Γ, and the percentage direct reaction contribution to the cross section, y_D, are presented in the first two columns of Table I. The error bars quoted for the coherence widths reflect uncertainties in the appropriate averaging interval, while those on y_D indicate limits assuming the effective number of open channels between $N_{\text{eff}} = 1$ to a maximum value of $(2I+1)/2$. Of particular interest, however, are the results of the cross-correlation analysis presented in the last three columns of Table I and in Fig. 8. The angular correlation within a given inelastic channel (diagonal elements of Table I and black squares of Fig. 8) are particularly strong: 0.67, 0.45, 0.46 for the 6.1, 7.0, 4.4 MeV channels, respectively. The cross-channel correlation is strong between the 6.1- and 7-MeV levels in ^{16}O while those between the 4.4-MeV state in ^{12}C and the two ^{16}O levels are quite small. It should be emphasized that this analysis measures the correlation averaged over the whole range of the data and not just near the resonance energies.

C. Angular distributions

The elastic and inelastic excitation functions of Figs. 4–7 provide strong evidence for the existence of several new intermediate structure resonances. In order to determine the spins of the resonances elastic and inelastic angular distributions were measured at center-of-mass energies corresponding to prominent resonancelike structures observed in the excitation functions. These en-

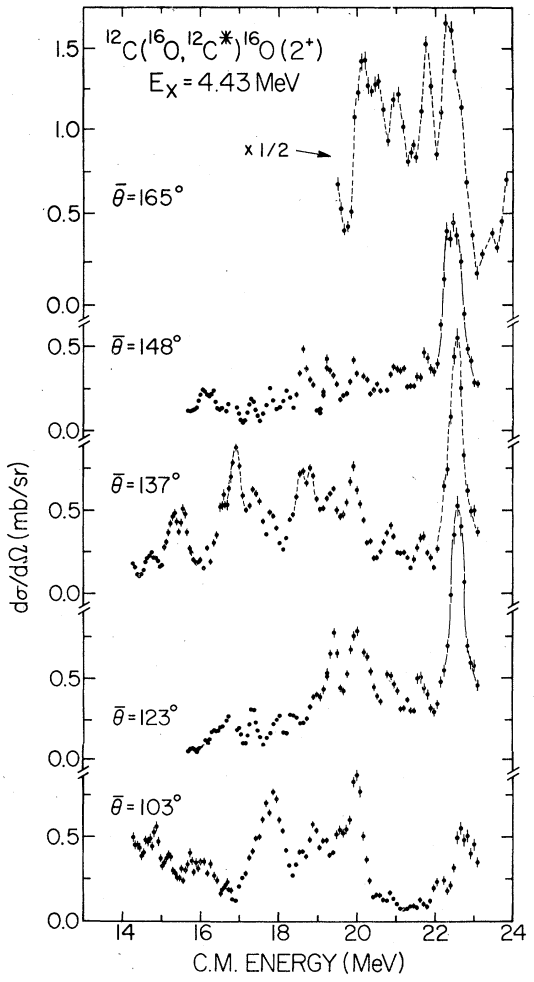

FIG. 6. Excitation functions for $^{12}C + ^{16}O$ inelastic to the 2^+ state at 4.43 MeV excitation in ^{12}C.

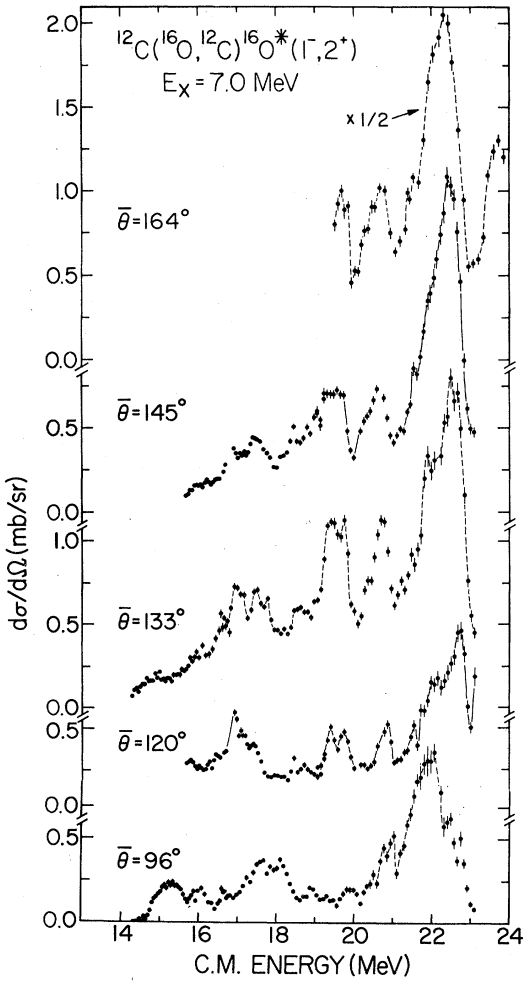

FIG. 7. Excitation functions for $^{12}C + ^{16}O$ inelastic scattering to the $(2^+, 1^-)$ doublet at 7 MeV excitation in ^{16}O.

ergies included 22.6, 22.0, 20.5, 19.7, and 13.6 MeV as well as 21.3 MeV which is a "nonresonant" energy for all of the observed inelastic channels. By assuming the existence of a single isolated resonance interfering with a direct background, fits to the elastic scattering angular distributions were obtained by adding a Breit-Wigner resonance in a given partial wave to an optical model background phase. In this approach the nuclear part of the elastic S-matrix element becomes

$$S_l = S_l^{\text{om}} + ie^{2i\delta_l}e^{2i\phi}\frac{\Gamma_i}{E - E_R - i\Gamma/2}, \quad (1)$$

where S_l^{om} is the background S-matrix element for the partial wave l, Γ_i is the elastic width, Γ is the total width, E_R is the resonance energy, ϕ is the relative mixing phase, and δ_l is the real part of the optical model phase shift. The optical model parameters used in this analysis were those obtained from fits to the gross structure of the $^{12}C + ^{16}O$ elastic scattering excitation functions of Ref. 20, and are listed as set I in Table II. Since the optical model underestimates the back angle cross section by ~2 orders of magnitude the error of double counting arising from this procedure is very small. The magnitude of the curves

TABLE I. Results of statistical analysis of the three inelastic scattering excitation functions. Γ is the average width of underlying compound states, Y_D the percentage of noncompound ("direct") reaction; the coefficients $\langle c_{ij} \rangle$ give the channel-channel correlations.

E_{ex} MeV	I^π	$\langle\Gamma\rangle$	Y_D %	$\langle C_{ij}\rangle$ 6.1	7.0	4.4
6.1	3^-	153 ± 15	92 ± 4	0.67	0.33	-0.09
7.0	2^+	195 ± 30	95 ± 2	0.33	0.45	0.11
4.4	2^+	135 ± 15	87 ± 6	-0.09	0.11	0.46

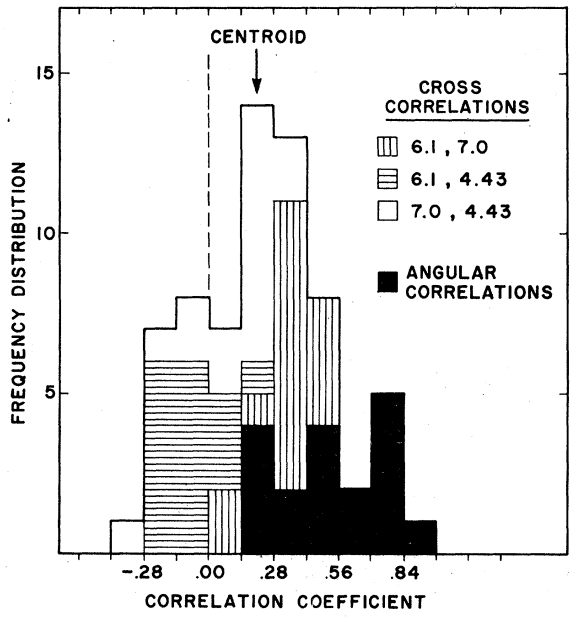

FIG. 8. Frequency distribution of cross correlation coefficients for inelastic channels in $^{12}C+^{16}O$ scattering. The different shadings represent correlations between particular channels as indicated.

fitted to the elastic angular distributions at large angles is strongly dependent upon the ratio Γ_i/Γ while the phase of the oscillations at far backward angles ($\theta_{c.m.} > 160°$) is almost uniquely determined by the resonant spin value. The relative mixing phase ϕ, between the optical model background and the resonant amplitude is the only free parameter in this approach. Its effect was to cause small shifts in the positions of the maxima and minima at center-of-mass angles between 100° and 150°. For all of the resulting fits to the data this phase was small ($0 \leq \phi \leq 30°$).

The elastic scattering angular distribution at $E_{c.m.} = 22.6$ MeV and fits to the data assuming resonant spins of $J = 13$, 14, 15, and 16 are presented in Fig. 9. The $J = 16$ fit is advanced in phase relative to the data at the crucial backward angles and produces one oscillation too many in the fit. On the other hand, fits with $J = 13$ are retarded in phase with one too few oscillations overall. $J = 15$ reproduces quite well the position of the maximum at 165° but gets progressively out of phase at smaller angles, with again one too many oscillations in the angular range 90°–160°. Assuming a resonant spin of $J = 14$, reasonable agreement with the data is obtained for all but the largest angles where the phase of the fit may be lagging behind that of the data. The results of these fits must be interpreted with caution, however, since there is no real indication of resonant behavior at 22.6 MeV in the elastic scattering correlation function of Fig. 3. The results in Fig. 9 may be interpreted as evidence that the dominant partial waves at this energy are $l = 14$ and $l = 15$.

At $E_{c.m.} = 22.0$ MeV, however, an elastic angular distribution may be expected to yield more interesting results since there is correlated structure at this energy in the elastic excitation function (Fig. 2) and in the correlation function of Fig. 3. In Fig. 10 elastic scattering angular distributions with fits for the assumed resonant spins $J = 15$ and 16 are presented. It is interesting that the pattern of the angular distribution changes abruptly with the appearance of an additional oscillation in the backward angle region at 22.0 MeV as compared to that at 22.6 MeV. The fit obtained with a resonance spin of $J = 15$ (top) agrees nicely in phase with the crucial most-backward oscillation and gives fairly good agreement over the entire angular region. The $J = 16$ fit (bottom) is slightly advanced in phase at the most backward angles. However, the quality of this fit compared to that of $J = 15$ is not poor enough to rule out the possibility of a resonant spin assignment of $J = 16$.

The elastic scattering angular distribution at $E_{c.m.} = 19.7$ MeV is presented in Fig. 11 along with fits assuming resonant spins of $J = 13$ and $J = 14$. The present data extend backward to include one more oscillation than those of Ref. 20 where a spin assignment of $J^\pi = 14^+$ was proposed using an identical analysis. The fit assuming $J^\pi = 14$ (top) reproduces the overall pattern of oscillations quite well but is slightly advanced in phase at the backward angles as compared to the data. On the other hand, the fit with $J = 13$ (bottom) gives good

TABLE II. Two sets of optical potentials which fit the elastic scattering. The two sets represent extreme cases of reasonable absorptive potentials.

	V (MeV)	r_o (fm)[a]	a_o (fm)	W (MeV)	r_i (fm)[a]	a_i(fm)
Set I	$7.5 + 0.4E_{c.m.}$	1.34	0.45	$0.4 + 0.125E_{c.m.}$	1.34	0.45
Set II	$7.5 + 0.4E_{c.m.}$	1.34	0.45	$-17 + 1.86E_{c.m.}$	0.81	0.80

[a] $R = r_{0,i}(A_1^{1/3} + A_2^{1/3})$.

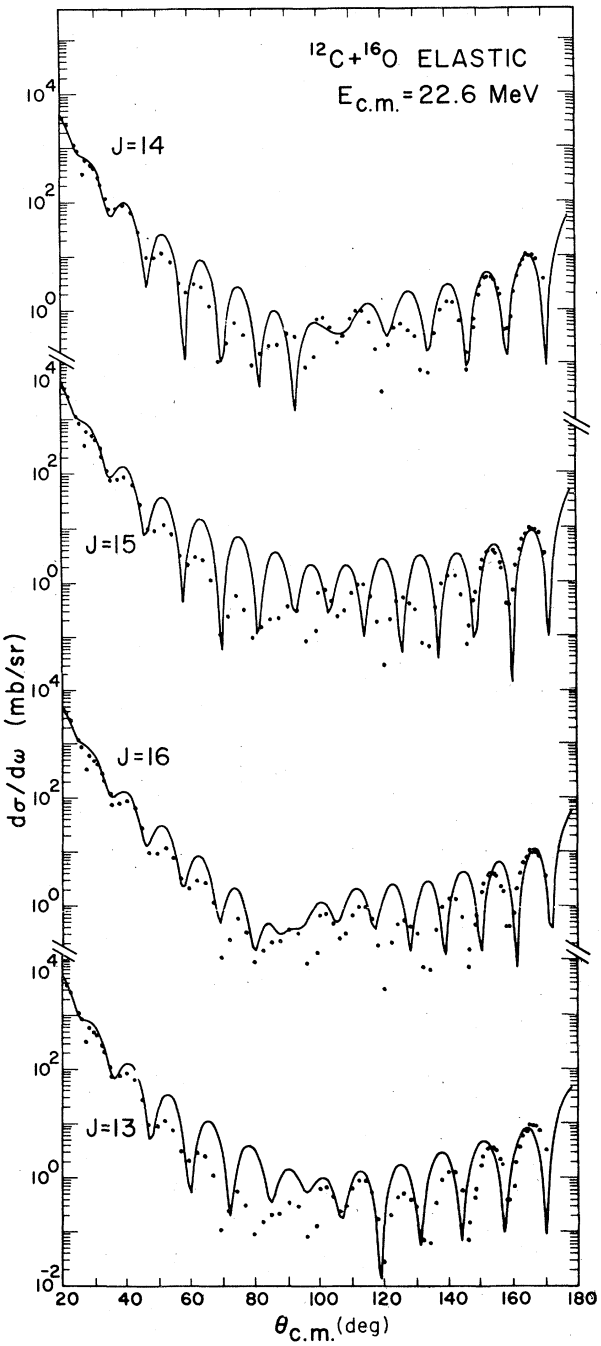

FIG. 9. Elastic scattering angular distributions at 22.6 MeV (c.m.) and fits assuming resonant spin of J = 13 to 16.

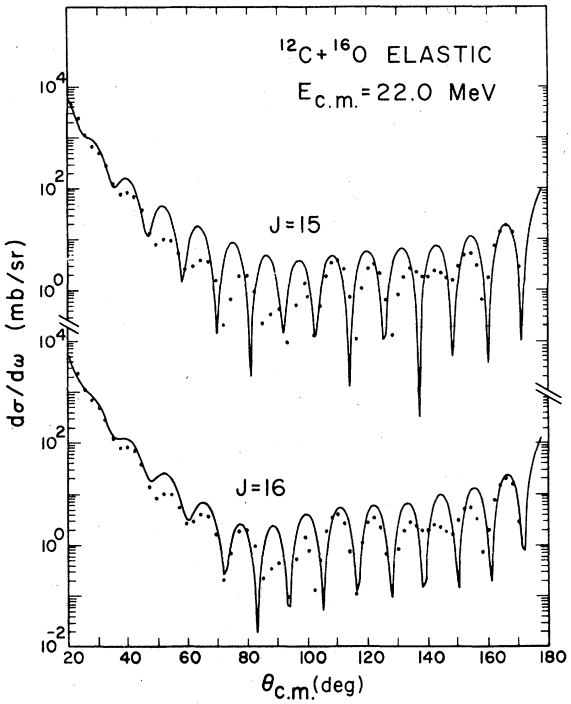

FIG. 10. Elastic scattering angular distribution at 22.0 MeV (c.m.) and fits assuming resonant spin of J = 15 and J = 16.

agreement at the backward angles and except in the angular range $85^\circ \lesssim \theta_{c.m.} \lesssim 125^\circ$ does a better overall job in fitting the data. For the crucial most-backward oscillation both fits do equally well with perhaps the $J = 14$ providing the better fit. This example emphasizes the care which must be exercised in deducing resonant spins (especially for high spins) from elastic scattering data. Even in this case, where the resonance is strongly evident over a broad range of angles, an unambiguous spin determination would be difficult were it not for the ancillary fact that the resonance is visible in the 90° excitation function of Ref. 20 ruling out odd values of J.

The elastic scattering angular distribution at $E_{c.m.}$ = 13.6 MeV is presented in Fig. 12 along with calculations for resonant spins of $J = 8$, 9, and 10. Since this resonance is also observed strongly in the elastic channel there should be no problem with interpretation. It is evident from the figure that agreement between calculation and data is obtained only with the spin assignment $J = 9^-$. Angular distributions just above and below the resonance exhibit a pattern more characteristic of P^2_{10}. Corroborative evidence for this assignment is obtained from analysis of the $\alpha + ^{24}Mg$ ground state transition data of Ref. 18 which is shown in Fig. 13. Using a coherent sum of two Legendre polynomials with complex coefficients, an acceptable fit is obtained only when the magnitude of the A_9 coefficient is much greater than that of A_8 or A_{10}.

Important information can be obtained from inelastic angular distributions taken on resonance, such as the total angle-integrated cross sections

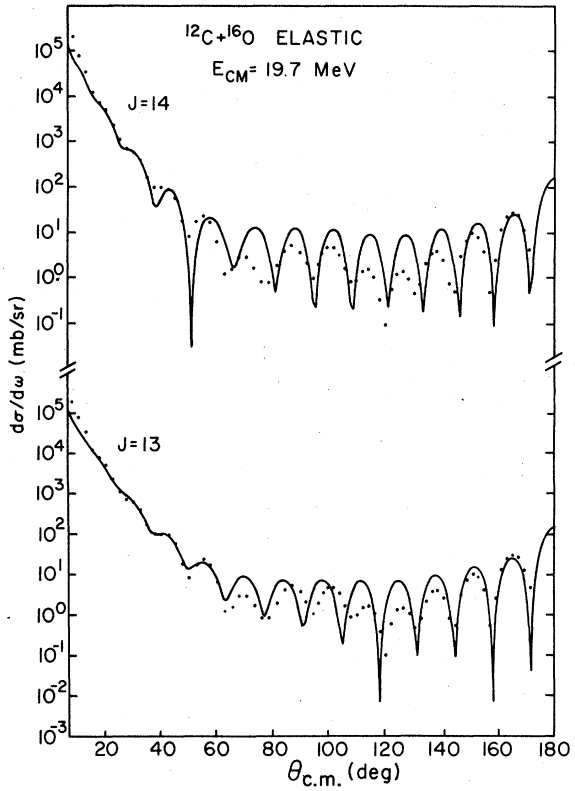

FIG. 11. Elastic scattering angular distribution at 19.7 MeV (c.m.) and fits assuming resonant spin of $J=13$ and $J=14$.

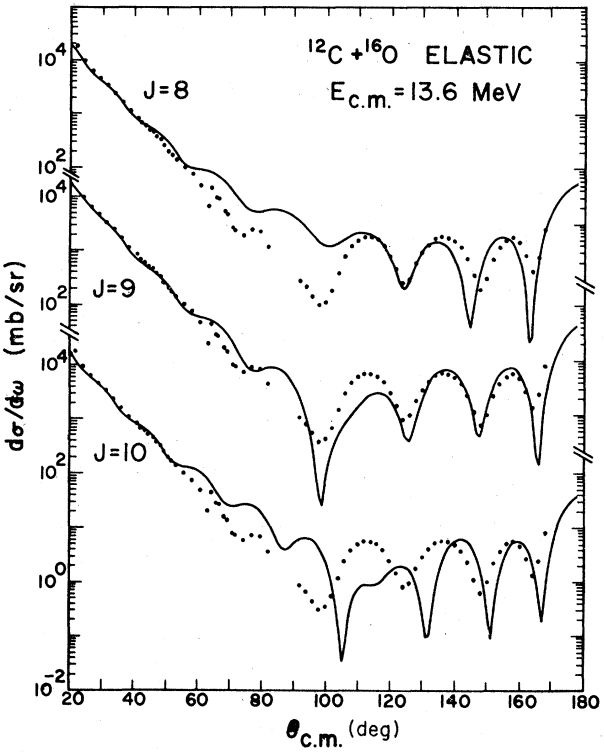

FIG. 12. Elastic scattering angular distribution at 13.6 MeV (c.m.) and fits assuming resonant spin of $J=8$, 9, and 10.

for specific inelastic channels. These provide much needed insight (via partial width information) as to which inelastic channels are most important in the resonance reaction mechanism. In addition, qualitative information concerning the resonant spin can be derived despite the fact that the final state spins are not zero. The inelastic angular distributions at $E_{c.m.}=22.6$, 21.3, 20.5, and 19.7 MeV are presented in Fig. 14 for scattering to the 2^+ state at 4.43 MeV in ^{12}C. Likewise Figs. 15 and 16 show the angular distributions for inelastic scattering to the $(3^-, 0^+)$ doublet at 6.1 MeV in ^{16}O and to the $(2^+, 1^-)$ doublet at 7.0 MeV in ^{16}O, respectively, for the same five center-of-mass energies. Only backward angles are included for most of the angular distributions in Figs. 15 and 16 due to the difficulty in accurately distinguishing the peaks at 6.1 and 7.0 MeV excitation in the angular region $60° < \theta_{c.m.} < 90°$ where the differential cross sections are smallest. The 4.43- and 6.1-MeV final state angular distributions contain a large amount of structure whereas in the 7.0-MeV data the oscillations are less pronounced. Comparing the 4.43- and 6.1-MeV state angular distributions to the elastic ones at the

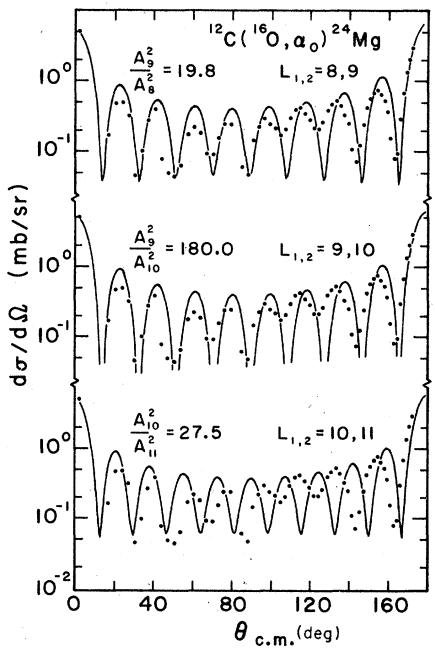

FIG. 13. Angular distributions from the $^{12}C(^{16}O, \alpha_0)^{24}Mg$ reaction taken from Ref. 18. The solid curves are fits assuming a scattering amplitude of the form $f(\theta) = A_{L1}P_{L1}(\cos\theta) + A_{L2}P_{L2}(\cos\theta)$ with $A_{L1, L2}$ complex.

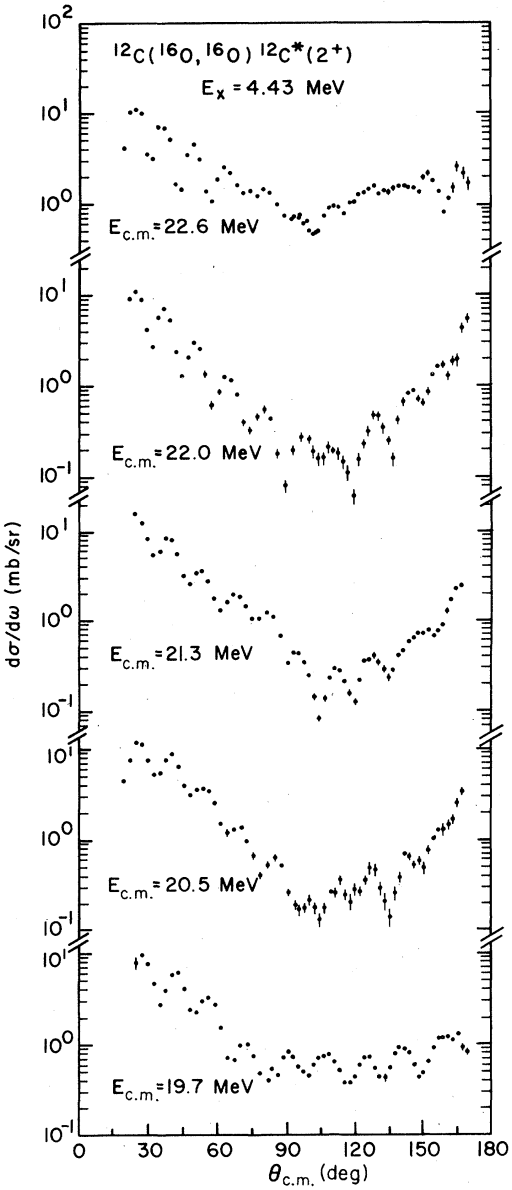

FIG. 14. Angular distributions for inelastic scattering to the 2^+ state at 4.43 MeV excitation in ^{12}C at several resonant energies and one nonresonant energy $E_{c.m.}$ = 21.3 MeV.

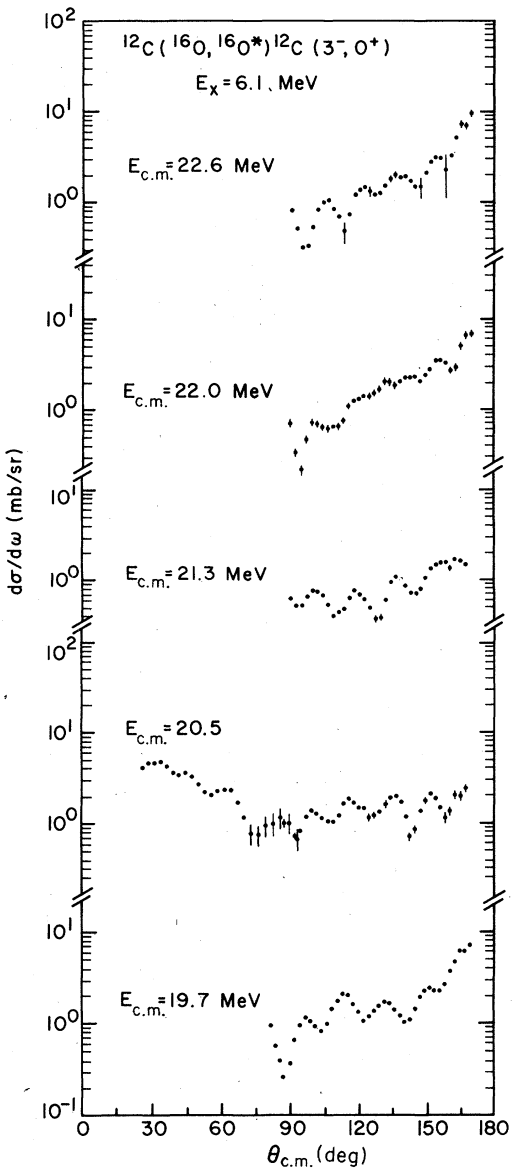

FIG. 15. Angular distributions for inelastic scattering to the $(3^-, 0^+)$ doublet at 6.1 MeV excitation in ^{16}O at several resonant energies and one nonresonant energy $E_{c.m.}$ = 21.3 MeV.

corresponding energies, it is obvious that lower values of the relative angular momentum L are needed if one were to fit the oscillations in the inelastic angular distributions assuming $d\sigma/d\Omega \sim |P_l(\cos\theta)|^2$. Thus, the angular momentum coupling of the final state spin is such that the inelastic excitation removes angular momentum from the relative motion.

IV. PARTIAL RESONANCE WIDTHS

In order to obtain complete information on partial widths for a given resonance, the resonance must be observed in the elastic channel. For this reason, only at $E_{c.m.}$ = 13.7, 19.7, and possibly at 22.0 MeV is it possible to derive tenable results on widths from the present experiment. Results presented for

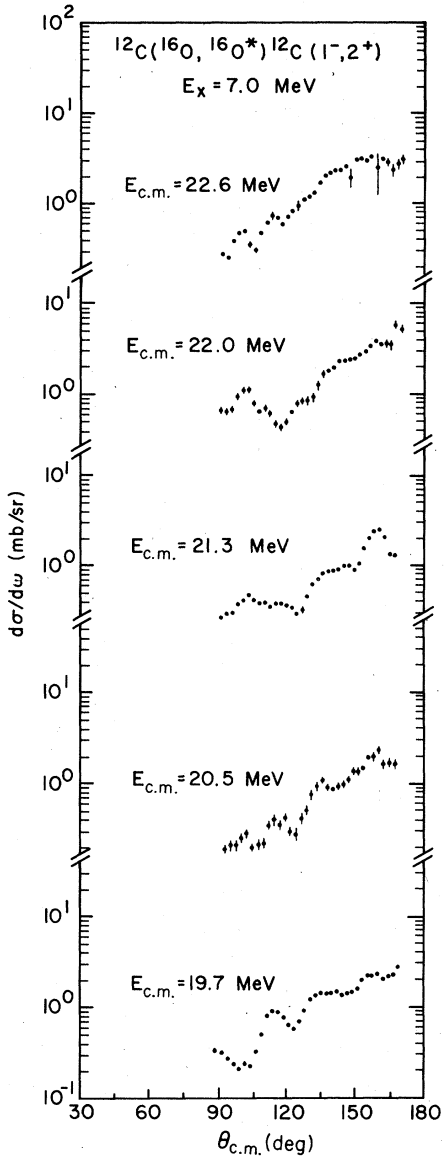

FIG. 16. Angular distributions for inelastic scattering to the $(2^+, 1^-)$ doublet at 7 MeV excitation in ^{16}O at several resonant energies and one nonresonant energy $E_{c.m.}$ = 21.3 MeV.

22.6 MeV are estimates based on an upper limit of 100 keV for the elastic width. The results are summarized in Tables III and IV and are discussed below in detail for the 19.7-MeV resonance.

An estimate of the single particle width is obtained from the width of the optical model potential resonance using the real part of the empirically determined $^{12}C + ^{16}O$ potential. We use again the energy dependent potential of set I in Table II. In the present analysis the depth of the potential at $E_{c.m.}$ = 19.7 MeV is increased by 8% from 15.4 to 16.6 MeV in order to shift the calculated $l = 14$ resonance to the experimentally observed energy. The resulting single particle width $\Gamma_{s.p.}$ = 1.5 MeV is four times larger than the experimentally observed width Γ = 380 keV.

TABLE III. Energies and experimental widths of strong inelastic resonances, along with spin assignment from analysis of elastic scattering. The single particle widths $\Gamma_{s.p.}$ have been computed with the empirical optical potential Set I of Table II.

$E_{c.m.}$ (MeV)	E_{exp} (keV)	J^π	Γ_{el}/Γ	$\Gamma_{s.p.}$ (OM)	$\Gamma_{el}/\Gamma_{s.p.}$
13.7	~100	9^-	0.25		
19.7	380	14^+	0.25 ± 0.05	1.5	6%
20.5	400				
22.0	500	$15^-(16^+)$	0.30 ± 0.05	1.8	8%
22.6	500		$0.22^{+0.05}_{-0.15}$		<7%

The elastic width is estimated from the fits to the resonant elastic scattering data. The ratio of the elastic width Γ_{el} to the total width Γ required to fit the magnitude of the 19.7-MeV cross section at backward angles is $\Gamma_{el}/\Gamma = 0.25 \pm 0.05$, and therefore Γ_{el} = 95 keV. This is 6% of the single particle width and results in a total resonant reaction width $\Gamma_R = \Gamma - \Gamma_{el}$ = 285 keV. The total peak resonant reaction cross section σ_R, for $l = 14$, is

$$\sigma_R = 4\pi\lambda^2(2l+1)\frac{\Gamma_{el}\Gamma_R}{\Gamma^2} = 106 \text{ mb}. \quad (2)$$

This amounts to 15% of the total reaction cross section and ~100% of the partial cross section for the $l = 14$ partial wave calculated with the optical model. The partial resonance widths Γ_i for inelastic scattering are determined from the relation

$$\Gamma_i \cong \frac{\sigma_i}{\sigma_R}\Gamma_R . \quad (3)$$

The resonant inelastic cross sections σ_i are estimated from the resonant inelastic scattering angular distributions of Figs. 15–17 by integrating from $\theta_{c.m.} = 90°$ to $\theta_{c.m.} = 180°$ and multiplying by 2. The results for σ_i and Γ_i are listed in the third and fourth columns in Table III. Integration of the data over the entire 180° angle range increases the cross sections typically by a factor 1.6. Since the forward hemisphere includes direct components we believe that the extraction of σ_i from the backward hemisphere is more valid and accurate to ±25%. This error includes allowance for possible nonresonant nondirect components.

Energy-independent reduced widths γ_i^2 can be calculated from the observed partial resonance widths in the various inelastic channels using the relation

TABLE IV. Cross sections and reduced widths for some inelastic resonances. Reduced widths ratios in column 5 are computed using penetrabilities with a reasonable range of matching radii, those in column 6 using optical model transmission coefficients with two sets of parameters taken from Table II. Errors on cross sections are estimated to ±25%.

Energy (MeV)	Channel	σ (mb)	Γ_i (keV)	γ_i^2/γ_{el}^2 ($R = 6.5 \pm 0.5\,f$)	γ_i^2/γ_{el}^2 T (OM)	ℓ
19.7	Elastic		95	1	1	14
	^{16}O (3$^-$)	22.3	60	$2.6^{+0.3}_{-0.6}$	3.6–5.2	11
	^{16}O (2$^+$)	11.8	32	12^{+7}_{-5}	20–25	12
	^{27}Si	2.6	7	0.15 ± 0.1	0.24	2
					1.8	4
	^{27}Al	9	24	$0.17^{+0.17}_{-0.10}$	0.40	2
				1.7 ± 0.6	1.40	4
22.0	Elastic		150	1	1	15
	^{16}O (3$^-$)	21.4	66	$1.0^{+0.01}_{-0.10}$	0.84–0.94	12
	^{16}O (2$^+$)	19	59	$5.4^{+2.3}_{-2.1}$	9.6–9.3	13
22.6	Elastic		$\leqslant$100	1	1	(15)
	^{16}O (3$^-$)	19.5	93	$1.9^{+0}_{-0.2}$	1.0–1.2	12
	^{16}O (2$^+$)	16.4	78	$7.9^{+3.7}_{-3.0}$	10.5–11.4	13
	^{12}C (2$^+$)	25.2	120	2.0 ± 0.1	1.3–1.4	13

$$\Gamma_i = \sum_l 2P_l\gamma_{il}^2 . \quad (4)$$

A sharp cutoff model for the nuclear surface leads to the well-known penetration factor

$$P_l = k_i R_i (F_l^2 + G_l^2)^{-1}, \quad (5)$$

where F_l and G_l are the regular and irregular Coulomb functions evaluated at the channel radius R_i. For the case of a diffuse nuclear surface the channel radius R is not well defined. To remedy this problem Michaud *et al.*[34] and Arima and Yoshida[35] suggest replacing the Coulomb functions (F_l and G_l) in the penetration factor with the wave functions $\bar{F}_l$ and $\bar{G}_l$ obtained from the radial wave functions of the optical potential. When this procedure is applied in the present case the resulting penetration factors $\bar{P}_l$ are still sensitive both to the radius and potential parameters used. Since our primary interest is to compare the elastic and inelastic widths and since the radius, although somewhat arbitrary, is the same for both channels we have simply used the conventional Coulomb wave functions. The resulting reduced widths are presented in Table IV with errors indicating the spread introduced by a reasonable choice of interaction radii, along with the partial waves assumed in the decay channels.

Included in Table IV are estimates of the cross sections and widths for the n+ ^{27}Si and p+ ^{27}Al channels at 19.7 MeV. The neutron decay of the 19.7-MeV resonances has been studied in detail by Sperr *et al.*,[23] who find that two states in ^{27}Si at $E_x = 15.37$ MeV and 17.04 MeV are strongly populated on—but not off—resonance. Angular distributions are consistent with a neutron angular momentum $l_n = 2$ to 4. Integrated cross sections were estimated from the curves of Ref. 23 and the corresponding widths are given in the table. Also shown are reduced widths computed for angular momenta $l = 2$ and 4 in the nucleon decay channels.

Somewhat more arbitrarily, reduced width ratios may also be estimated using optical model transmission factors in lieu of the standard penetration factors. These transmission factors were computed for two different empirical potentials[25] listed in Table II. The two imaginary potentials of set I and set II are reasonable extreme limits which still fit elastic scattering. The ratios so obtained are listed in the sixth column in Table IV. Interestingly, these ratios agree quite well with

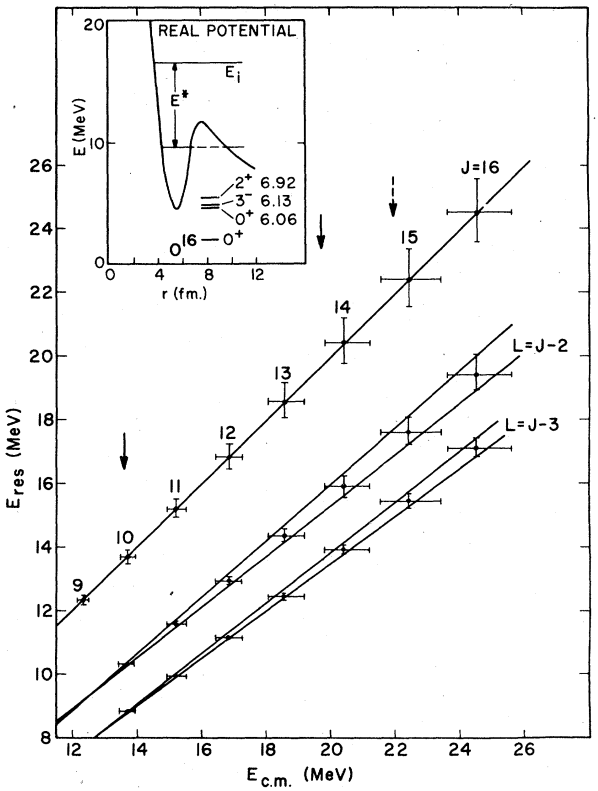

FIG. 17. Schematic of double resonance mechanism (insert). Top curve is the trajectory of shape resonances in the real part of the empirical optical potentials. Lower curves give position of quasibound levels in $l=J-2$ and $l=J-3$ potentials.

the penetrability results within the range provided by admissible channel radii. We note parenthetically that this is not the case if the Yale potential as parametrized by Gobbi[21] is used.

The uncertainties in these reduced width ratios are large. Nevertheless, it is clear from Table IV that the inelastic channels dominate the structure of these resonances. In particular, any theoretical model of the resonance mechanism will have to explain the particularly large widths of the 2^+ state at 6.92 MeV excitation in ^{16}O.

V. DISCUSSION

The properties of the observed resonances at 13.6, 19.7, 22.0, and 22.6 MeV may now be interpreted in terms of various proposed models.

First, we recall that the strong angular cross correlation in each of the inelastic channels persists over the entire measured range of angles ($90° \leq \theta_{c.m.} \leq 165°$). This range is much larger than the coherence width $\Delta\theta_{c.m.} \approx 6°$ expected if all partial waves participate in the reaction. Thus only a few partial waves are involved which is indicative of a doorway mechanism. On the other hand, the cross-channel correlations, especially those involving the ^{12}C (2^+) channel, are much weaker.

From elastic scattering angular distributions the spin assignments $J^\pi = 9^-$, 14^+, 15^- (16^+) are assigned to the resonances at 13.6, 19.7, and 22.0 MeV. At 22.6 MeV the predominant partial waves are 14 and 15. In the absence of a strong elastic resonance neither spin value can be unambiguously assigned to the 22.6-MeV resonance, although an assignment of $J^\pi = 14^+$ has been made by the Saclay group.[36] In fact, the present data and those of Ref. 36 at large angles ($\theta_{c.m.} \cong 165°$) agree better with $J^\pi = 15^-$.

Additional resonances have been reported, notably in the $^8Be + ^{20}Ne$ channel, which appear only weakly in the present inelastic excitation functions. Table V summarizes the energies of weak resonantlike structures observed in the present work along with known correlations in other exit channels. The evidence for these inelastic channel resonances, however, is much weaker than that for the resonances listed in Table III. Notably, a resonance at $E = 20.8$ MeV reported[36] from elastic scattering data at $\theta_{c.m.} = 166°$ with a spin attribution of $J^\pi = 13^-$ also appears in our 7.0-MeV excitation function data and perhaps in the elastic and 4.43-MeV excitation functions as well. A peak is also evident at 20.75 MeV in the fusion data of Kolata *et al.*[37] James *et al.*[38] have reported a $J^\pi = 12^+$ resonance in the $^8Be + ^{20}Ne$ channel at 19.92 MeV where there is a prominent anomaly in our ^{12}C (2^+) inelastic scattering data and which they clearly distinguish from the 19.7-MeV $J^\pi = 14^+$ resonance. In addition to peaks in

TABLE V. Energies of weak or weakly correlated anomalies observed in the inelastic channels of this work (*) and other work, where known. Channels A, B, C, D, π indicate elastic scattering and inelastic scattering to the 6.13, 7.0, 4.43, and 6.05 MeV states, respectively. Channel f indicates fusion.

E (MeV)	Channel	Ref.
15.9	A; (B)	36; *
16.5	A; B	36; *
17.9	A; B; α	(*, 36, 21); *; 52
19.0	B	*
19.4	C; (D)	*; *
19.9	D; ^8Be	*; 38
20.5	B	*
20.8	A; C; D; f	(*, 36); *; *; 37
21.6	A; C; D; f	(*, 36); *; *; 37
23.8	A; B; C; D; π	(*, 36); *; *; *; 50

the fusion cross section at 22.0, 20.75, and possibly ~22.7 MeV, there is also a peak at ~21.5 MeV, very close to the energy of peaks in our 4.4- and 7-MeV inelastic scattering data. Before discussing these data further we note again that due to the high spins involved in these resonances spin assignments are often uncertain by one unit unless a measurement at $\theta_{\text{c.m.}} = 90°$ is made and may be meaningless unless the resonance is observed strongly in the channel from which the resonant spin is inferred.

The spin values obtained in this work for the strong resonances at 13.6 ($J^\pi = 9^-$), 19.7 (14^+), and 22.0 MeV (15^-) are all within one unit of the grazing angular momenta $l_g = 10$, 13, and 14, respectively. The same holds for most other reported resonances.[39] Associated with the grazing angular momenta are standing waves in the real part of the optical ion-ion potential. These are shown in Fig. 17 where the top curve gives the c.m. elastic channel energies of shape resonances computed using the empirical optical potential with $W \equiv 0$. The energy-dependent potential given in Table II was used with parameters which fit the elastic scattering. When standing wave resonances were recently reported by Cormier *et al.*[40] in the $^{12}C + ^{12}C$ system, this energy-dependent potential gave the best fit to the observed sequence of peak energies. The half-widths of the shape resonances indicated by bars in Fig. 17 are defined by the energies at which the elastic phase shift passes through 45° and 135°. The positions of the best established resonances from the present work are indicated by arrows. We note that the 19.7-MeV ($J^\pi = 14^+$) and 22.0-MeV (15^-) resonances occur quite close to the respective standing waves computed from the potential, whereas the 9^- resonance at 13.7 MeV lies in the 10^+ standing wave region. The reported $J^\pi = 12^+$ resonance at 19.92 MeV misses the pattern seriously, i.e., by 2 units.

It is apparent again from Fig. 17 that the experimentally observed resonance widths are much smaller than those of the computed standing wave resonances even with $W \equiv 0$. It can also be concluded from the reduced width ratios in Table IV that the reaction is dominated by the inelastic channels. At 19.7 and 22.0 MeV the summed inelastic cross section for the 6.1- and 7-MeV levels accounts for $\geq \frac{1}{3}$ of the resonant reaction cross section. At 22.6 MeV the sum of all inelastic channels amounts to ~73% of the estimated resonant reaction cross section.

The double-resonance mechanism[29] explains intermediate resonances above the barrier in terms of a strong (but not too strong) coupling of the elastic channel to the low-lying collective 2^+ and 3^- excitations in ^{12}C and ^{16}O. These are just the inelastic channels observed in the present experiment, which, therefore tests this simple and appealing model directly. The inset of Fig. 17 taken from Scheid *et al.*[29] depicts the mechanism. The incident ion enters the effective ion-ion potential above the barrier with an energy E_i and is trapped into the well by exciting one or both ions to an energy E^*. Resonances occur when the energy $E_i - E^*$ matches that of a lower trapped (quasibound) state in the well.

This model immediately encounters a serious problem. There are strong indications on experimental[41] and theoretical[42] grounds that the effective ion-ion potential is energy dependent, becoming deeper with increasing relative ion energy. It seems then plausible that the molecular eigenstates must be calculated in the potential depth appropriate for the energy contained in molecular motion. This means in most cases that the final (inelastic) resonance is not significantly more bound than the initial (elastic) one, and using this prescription one does not obtain narrow resonances by the double-resonance mechanism.

With this reservation in mind we have computed at each excitation energy the molecular eigenstates using the potential of the elastic channel. The resulting kinematic and angular momentum matching conditions imposed by the double-resonance mechanism are illustrated in Fig. 17. As a function of excitation energy $E_{\text{c.m.}}$ (which specifies the potential depth), the energies of the elastic standing wave $L = J$ and those of the lower waves $L = J - 2$ and $J - 3$ are plotted. It can be seen that with this potential choice the lower resonances are indeed narrower. For example, a quasibound level appears in the $L = J - 3$ curve about 6.5 MeV below the position where the $L = 14$ wave resonates in the entrance channel. This suggests that inelastic scattering to the 3^- state in ^{16}O at $E^* = 6.13$ MeV fulfills the matching conditions of the double-resonance mechanism and that an intermediate resonance should appear at this energy in this channel. Indeed the $E_{\text{c.m.}} = 19.7$-MeV resonance is observed strongly in the 3^- state excitation function. However, as Fig. 17 shows, the $L = J - 2$ curve is also well matched at this energy with excitation of the 4.43-MeV 2^+ state in ^{12}C but this channel does not in fact resonate at 19.7 MeV. There is evidence, however, for weaker resonances in this channel at 19.4 and 19.9 MeV. On the other hand, the 2^+ state at 6.93 MeV in ^{16}O is badly mismatched and yet resonates strongly.

At 22.6 MeV the ^{12}C (4.43) and ^{16}O (6.13) channels resonate and are indeed well matched to an $L = 15$ entrance channel wave. But again the strong resonance effect in the ^{16}O (6.93, 2^+) curve

is not explained by the simple double-resonance model.

If all of the correlated intermediate structure observed in the ^{12}C (4.43) and ^{16}O (6.1 and 7.0) excitation functions is considered, it is difficult to explain these phenomena in terms of the simple double-resonance mechanism. In particular it seems that the 7 MeV excitation is always seriously mismatched yet it resonates strongly.

The most striking feature of the inelastic excitation functions is the consistent appearance of doublets. An extension of the double-resonance mechanism as proposed by Abe *et al.*[43] which includes all possible angular momentum couplings and additional inelastic channels naturally produces more numerous resonances of each spin value. Including only the coupling to the 3^- state in ^{16}O and the 2^+ state in ^{12}C and using a modified optical potential Kondo *et al.*[44] have generated preliminary coupled channel fits which reproduce the general features of the 3^- and 2^+ inelastic excitation functions of Fig. 4 and 6; in particular, they obtain double-peaked resonances of intermediate width (~200–500 keV). They predict nine resonances between 16- and 23-MeV c.m. incident energy, three each of spin 13^-, 14^+, and 15^- overlapping in energy. Further spin determination of the inelastic peaks is required to test this model decisively.

A more fundamental attempt to compute the eigenstates of the $^{16}O+^{12}C$ system has recently been published by Baye and Heenen.[45] They compute the "molecular eigenstates" using microscopic wave functions for the ^{12}C and ^{16}O ground states totally antisymmetrized, and obtain elastic resonances which often lie close in energy to the reported ones. For instance a $J^\pi = 9^-$ resonance is predicted at 12.3 MeV, 11^- at 11.2 and 15.2 MeV, 12^+ at 13.53 and 16.9 MeV, 13^- at 15.94 and 19.0 MeV, 14^+ at 19.7 MeV, and 15^- at 22.2 MeV. On the other hand, the computed widths are in all cases too large and it is clear that the predicted resonances, for $L \geq 8$, correspond closely to the optical potential standing waves computed in Fig. 17. Explanation of the observed narrow intermediate structure clearly requires more intrinsic degrees of freedom. This is evidenced by the fact that in all cases observed in the present work the elastic channel is *dominated* by the inelastic ones. Accordingly, to use all resonances observed in nonelastic channels to substantiate molecular level schemes computed only for elastic channels appears of questionable value.

Several attempts have been made to group reported resonances into rotational bands, most recently by Resmini *et al.*[46] Although such fits leave the question of the intrinsic structure of the bands open, such classification seems premature in view of the multiplicity of reported resonances and the paucity of firm spin assignments.

An alternative mechanism capable of providing additional degrees of freedom to the resonating system is the α-particle exchange[16,21] model. This process populates the same low-lying excitations in ^{12}C and ^{16}O as inelastic scattering, but the various final states will be populated with differing strengths depending on the structure of the state and the excitation mechanism. For example, the low-lying 3^- state in ^{16}O and 2^+ state in ^{12}C are known to be quite collective with large $B(EL)$ values from inelastic α scattering.[47] On the other hand, the $(1^-, 2^+)$ states at 7 MeV in ^{16}O would appear to have a structure which hinders inelastic scattering, the 1^- state because it is an isoscalar $E1$ excitation and the 2^+ state because it is basically a 4p-4h state. The ^{16}O (2^+) state then would appear to be favored by α transfer, and the strong resonant observation of it as reported in a high-resolution experiment[48] would then favor the α-particle exchange model. Unfortunately, the distinction between the two excitation mechanisms is not so clearcut. In inelastic α-particle scattering[47] the 6.93 2^+ state in ^{16}O exhausts about 10% of the $E2$ sum rule, the same amount as the 3^- state does for the $E3$ excitation. So both states have about the same degree of collectivity. Conversely, it is well known that the 1p-1h 3^- state is about as strong in α transfer reactions as the 6.93-MeV 2^+ state. In fact there appears to be a general rule connecting the multipole collectivity and α transfer strength.[49] Unfortunately these higher excitations have not been included so far in the double-resonance model to check if the large resonant effect in the 6.93-MeV state could be quantitatively explained without invoking α transfer.

A more stringent test appears to be the excitation of the second (deformed) 0^+ state at 6.05 MeV relative to the 3^- state. The 0_2^+ state has an inelastic excitation cross section about 1/100 of that of the 3^- state yet appears strongly in the α transfer on ^{12}C. The excitation of this state is the subject of a separate paper.[50] We only note here that this experiment also leaves the nature of the reaction process in doubt, although we have observed strong resonances in the 0_2^+ channel at energies above $E_{c.m.} = 20$ MeV.

VI. CONCLUSIONS

This work was begun with the hope that the appealingly simple double-resonance mechanism would be borne out leading to a structural under-

standing of the intermediate heavy ion resonances. The data do not support this model, at least not in its simplest form. The spectrum of resonances is much too rich and obviously involves many degrees of freedom. However, it must be noted that the model predictions are potential dependent. Perhaps the use of other potentials such as the deep potential of Satchler[51] may yield different results. The conclusions which may be drawn from this work are summarized as follows:

(i) The inelastic channels in the $^{12}C+^{16}O$ system show a great deal of nonstatistical resonances of a width intermediate between Ericson fluctuations and ion-ion potential resonances.

(ii) Only a very few angular momenta in the formative channel contribute to the inelastic channels. Individual structures have a unique spin assignment which are within one unit of the grazing angular momentum or the standing wave resonances.

(iii) To the extent that reduced widths may be defined inelastic channels dominate the structure of the observed resonances, both relatively (compared to the elastic channel) and absolutely, i.e., in terms of the total resonant reaction cross section.

(iv) The emerging picture of at least the present narrow resonances is that of eigenstates which are populated through an "l window" or doorway (perhaps "molecular resonances" in the ion-ion potential) and which are structurally only one or two steps removed from the entrance channel. The additional excited degrees of freedom provide the increased lifetime of the states.

This last point is clearly most interesting even though the nature of the nuclear degrees of freedom is not yet known. Indications point toward α-particle exchange. In any case the system does exhibit eigenstates in which the two constituent nuclei are almost preserved. Intuitively, we expect that such states should have a large moment of inertia and follow an $\sim l(l+1)$ (i.e., peripheral) sequence. However, one must be very cautious in the interpretation of observed resonances. Since the reduction factor associated with an angular momentum mismatch with the elastic channel is dramatic for a heavy ion reaction, it could well be that there exists a rich spectrum of eigenstates which do not happen to lie near a doorway state and therefore are not observed.

---

†Work supported in part by the National Science Foundation.

*Present address: Physics Department, University of Notre Dame, Indiana.

[1]E. Almqvist, D. A. Bromley, and J. A. Kuehner, Phys. Rev. Lett. 4, 515 (1960); D. A. Bromley, J. A. Kuehner, and E. Almqvist, Phys. Rev. 123, 878 (1961).

[2]J. R. Patterson, B. N. Nagorka, G. D Symons, and W. M. Zuk, Nucl. Phys. A165, 545 (1971); B. N. Nagorka, G. D. Symons, W. M. Zuk, and J. R. Patterson, Nature Phys. Sci. 231, No. 18, 17 (1971).

[3]J. R. Patterson, H. Winkler, and C. S. Zaidens, Astrophys. J. 157, 367 (1969).

[4]M Mazarakis and W. E. Stephens, Astrophys. J. 171, 197 (1972); Phys. Rev. C 7, 1280 (1973).

[5]H. Spinka and H. Winkler, Nucl. Phys. A233, 456 (1974).

[6]Z. Basrak, R. Auger, B. Fernandez, J. Gastebois, and N. Cindro, J. Phys. Lett. 37, L131 (1976).

[7]K. A. Erb, R. R Betts, D. L. Hanson, M. W. Sachs, R. L. White, P. P. Tung, and D. A. Bromley, in Proceedings of the Symposium on Macroscopic Features of Heavy Ion Collisions, ANL Report No. PHY-76-2, 1976 (unpublished).

[8]H. Voit, G. Ischenko, F. Siller, and H. D. Helb, Nucl. Phys. A179, 23 (1972).

[9]M. L. Halbert and K. Nagatani, Bull. Am. Phys. Soc. 17, 530 (1972).

[10]D. L. Hansen, R. G. Stokstad, K. A. Erb, C. Olmer, M. W. Sachs, and D. A. Bromley, Phys. Rev. C 9, 1960 (1974).

[11]H. Vogt and H. McManus, Phys. Rev. Lett. 4, 518 (1960).

[12]R. H. Davis, Phys. Rev. Lett. 4, 521 (1969).

[13]B. N. Nagorka and J. O. Newton, Phys. Lett. 41B, 34 (1972); J. Y. Park, W. Scheid, and W. Greiner, Phys. Rev. C 10, 967 (1974).

[14]B. Imanishi, Phys. Lett. 27B, 267 (1968); Nucl. Phys. A125, 33 (1969).

[15]Y. Kondo, T. Matsuse, and Y. Abe, in *Proceedings of the Conference on Clustering Phenomena in Nuclei, Univ. of Maryland, College Park, 1975*, edited by D. A. Goldberg, J. B. Marion, and S. J. Wallace (Univ. of Maryland, College Park, Maryland, 1975).

[16]G. Michaud and E. W. Vogt, Phys. Lett. 30B, 85 (1969); Phys. Rev. C 5, 350 (1972).

[17]O. Krause, W. Scheid, and W. Greiner, Nukleonika 19, 267 (1974).

[18]M. L. Halbert, F. E. Durham, and A. Van der Woude, Phys. Rev. 162, 899 (1967).

[19]R. H. Siemssen, in Proceedings of the Symposium on Heavy Ion Scattering [ANL Report No. 7837, 1971 (unpublished)], p. 145.

[20]R. E. Malmin, R. H. Siemssen, D. A. Sink, and P. P. Singh, Phys. Rev. Lett. 28, 1590 (1972).

[21]R. G. Stokstad, D. Shapira, L. Chua, P. Parker, M. W. Sachs, R. Wieland, and D. A. Bromley, Phys. Rev. Lett. 28, 1523 (1972); D. Shapira, R. G. Stokstad, M. W. Sachs, A. Gobbi, and D. A. Bromley, Phys. Rev. C 12, 1907 (1975).

[22]E. R. Cosman, A. Sperduto, T. M. Cormier, T. N. Chin, H. E. Wegner, M. F. Levine, and D. Schwalm, Phys. Rev. Lett. 29, 1341 (1972).

[23]P. Sperr, D. Evers, A. Harasim, W. Assmann, P. Konrad, K. Rudolph, G. Denhofer, and C. Ley,

Phys. Lett. 57B, 438 (1975).
[24]J. P. Schiffer, Nucl. Phys. 46, 246 (1963).
[25]R. E. Malmin (thesis), Argonne Physics Division Report No. PHY-1972F, 1972 (unpublished).
[26]L. R. Greenwood, K. Katori, R. E. Malmin, T. H. Braid, J. C. Stoltzfus, and R. H. Siemssen, Phys. Rev. C 6, 2112 (1972).
[27]U. Facchini and E. Saetta-Menichella, Energ. Nucl. 15, 54 (1968). The range in ρ values corresponds to values obtained from using the radius parameters $r_0 = 1.3 \pm 0.1$ fm for the moment of inertia in the Fermi gas model.
[28]H. Feshbach, J. Phys. 37, C5-177 (1976) and references therein.
[29]W. Scheid, W. Greiner, and R. Lemmer, Phys. Rev. Lett. 25, 176 (1970); H. J. Fink, W. Scheid, and W. Greiner, Nucl. Phys. A118, 259 (1972).
[30]P. A. Moldauer, Phys. Rev. Lett. 18, 249 (1967).
[31]T. Ericson, Phys. Rev. Lett. 5, 430 (1960); Phys. Lett. 4, 258 (1963); Ann. Phys. (N.Y.) 23, 390 (1963).
[32]R. E. Malmin, J. W. Harris, and P. Paul, Bull. Am. Phys. Soc. 18, 134 (1973); R. E Malmin, *ibid.* 19, 1090 (1974); R. E. Malmin and P. Paul, in *Proceedings of the Conference on Clustering Phenomena in Nuclei, Univ. of Maryland, College Park, 1975.*
[33]J. D. A. Roeders, thesis, Univ. of Groningen, 1971 (unpublished).
[34]G. Michaud, L. Scheck, and E. W. Vogt, Phys. Rev. C 1, 864 (1970); E. Vogt, G. Michaud, and H. Reeves, Phys. Lett. 19, 570 (1965).
[35]A. Arima and S Yoshida, Nucl. Phys. A129, 474 (1974).
[36]P. Charles, F. Auger, I. Badawy, B. Berthier, M. Dost, J. Gastebois, B. Fernandez, S. H. Lee, and E. Plagnol, Phys. Lett. 62B, 289 (1976).
[37]J. J. Kolata, R. M. Freeman, F. Haas, B. Heusch, and A. Gallman, Phys. Lett. 65B, 333 (1976).
[38]D. R. James, G. R. Morgan, N. R. Fletcher, and M. B. Greenfield, Nucl. Phys. A274, 177 (1976).
[39]P. Taras, G. Roo, N. Shulz, J. V. Vivier, B. Haas, J. C. Merdinger, and S. Laundsberg, Phys. Rev. C 15, 83 (1977).
[40]T. M. Cormier, J. Applegate, G. M. Berkowitz, P. Braun-Munzinger, P. M. Cormier, J. W. Harris, C. J. Jachcinski, and L. Lee, Phys. Rev. Lett. 38, 940 (1977).
[41]R. H. Siemssen, H. T. Fortune, R. E. Malmin, A. Richter, J. W. Tippie, and P. P. Singh, Phys. Rev. Lett. 25, 536 (1970); R. H. Siemssen, in *Nuclear Spectroscopy and Reactions*, edited by J. Cerny (Academic, New York, 1974).
[42]U. Mosel, Part. Nucl. 3, 297 (1972); U. Mosel, in Proceedings of the Symposium on Macroscopic Features of Heavy Ion Collisions [ANL Report No. PHY-76-2, 1976 (unpublished)].
[43]Y. Abe, in *Proceedings of the Conference on Clustering Phenomena in Nuclei, Univ. of Maryland, College Park, 1975* (see Ref. 15), p. 500.
[44]Y. Kondo, T. Matsuse, and Y. Abe, in *Proceedings of the Conference on Clustering Phenomena in Nuclei, Univ. of Maryland, College Park, 1975* (see Ref. 15), p. 280; T. Matsuse, Y. Kondo, and Y. Abe, report (unpublished).
[45]D. Baye and P. H. Heenen, Nucl. Phys. A283, 176 (1977).
[46]F. G. Resmini, F. Soga, and H. Kamitsubo, Phys. Rev. C 15, 2241 (1977).
[47]K. T. Knopfle, G. J. Wagner, H. Brener, M. Ragge, and C. Mayer-Boericke, Phys. Rev. Lett. 35, 779 (1975); M. N. Harakeh, A. R. Arends, M. J. A. Voigt, A. G. Drentgi, S. Y. vanderWerf, and A. van der Wonde, Nucl. Phys. A265, 189 (1976).
[48]D. Shapira, R. M. DeVries, R. N. Boyal, and M. R. Clover, Bull. Am. Phys. Soc. 21, 553 (1976).
[49]D. Kurath and I. S. Towner, Nucl. Phys. A222, 1 (1974).
[50]R. E. Malmin, Fide Kahn, and P. Paul (unpublished).
[51]G. R. Satchler, Nucl. Phys. A279, 493 (1977).
[52]D. Branford, J. O. Newton, J. M. Robinson, and B. N. Nagorka, J. Phys. A7, 1193 (1974).